

THE STUDY OF CORONAL MASS EJECTION CYCLES USING THE AUTOREGRESSIVE MODELING

Muhammad Fahim Akhter¹, Danish Hassan², Shaheen Abbas¹

¹Mathematical Sciences Research Centre, Federal Urdu University of AS&T, Karachi

²Department of Applied Sciences, National Textile University Karachi Campus

KEYWORDS	ABSTRACT
Coronal Mass Ejection, Green Line Corona, Stochastic Models, ARIMA Model, ACF, PACF	The Sun produces a fair amount of solar energy caused by the different solar activities that affect the terrestrial environment. The lowest part of the sun's atmosphere is photosphere gases that can be recognized by the disk of the sun and above parts are the chromospheres and corona. The three parts of the structure of the sun's atmosphere crucial to understand the nature of solar activities. The analysis of the study segregated monthly cyclic data of green line emission corona 530.03λ nanometers by appropriate stochastic models. After identifying stationary of each cycle along with total data is observed and generate autoregressive AR (p), MA (q) and ARIMA (p, d, q) models have revealed a linear difference and ARMA for a total span based on minimization of Akaike information criterion and Schwarz Bayesian criterion. The parameters are examined by ACF and the PACF for different cyclic duration of Corona from 1944 to 2008. The models (0,1,1), (1,1,1) and (2,1,0) for cycles and (1,0,1) for total time series data were found the significance. The models obtained in this paper may be useful to understand and forecast the Coronal time series data.

INTRODUCTION

The Coronal Mass Ejection (CME) is an important phenomenon of the solar activity. The possible departures of CMEs explosion are in the Sun's Corona (Howard, 2006; Ebert, McComas, Elliott, Forsyth & Gosling, 2009). Solar eruption thrown into space at speed range from a few hundred to 2000 km/s of magnetic gas (Gopalswamy, Yashiro, Kaiser, Howard & Bougeret, 2001; Ebert et al., 2009). The sun's atmosphere typically refers to all the regions above the photosphere. Solar atmosphere separates into three layers, the photosphere, chromosphere, Corona on basis of temperature, density and composition. The lowest layer is photosphere and above the photosphere lie chromospheres and the Corona (Akhter, Abbas & Hassan, 2019). The Corona (Latin for crown) is shine brightly with reflected light. A circle of light around the sun at the time of solar eclipse (Akhter, Abbas & Hassan, 2018). The solar Corona can be seen when the moon is blocked out the photosphere.

The solar Corona has very high temperatures of order in millions of degrees (Prabhakar, Raju & Chandrasekhar, 2013). The first spectrum of the green line spectrum 530.3nm discovered by two American astronomers Harkness and Young during a full solar eclipse in 1869 but figure was not clear (Schwenn, Inhester, Plunkett, Epple, Podlipnik, Bedford & Lamy, 1997; KP, 2014). In this connection, the Corona has number of components K-Corona (kontinuierlichesspektrum), F-Corona (Fraunhofer), E-Corona (Emission) and T-Corona (Thermal). E-Corona (Emission) is composed of the line emission of visible to EUV (emission of ultra violate) due to various atoms and ions in the Corona. It contains many forbidden line transitions, therefore it contains many polarization states for real utilization. Some of strongest lines in this way are FeXIV 530.3nm (green-line; visible),

H- α at 656.3 nm (visible) and Lyman- α 121.6 nm (UV) (Akhter et al., 2018 and Akhter et al., 2018).

The green line emissivity which is due to forbidden transition of the FeXIV ion, peaks in temperature of about 2×10^6 (Wang, Sheeley, Hawley, Kraemer, Brueckner, Howard & Schwenn, 1997) for comparison the red line 637nm FeX ion has its maximum emissivity at the temperature around 10^6 K. The green line Coronal emission is the brightest of all emissions in visible spectrum range (Schwenn et al., 1997; wang et al., 1997; Mariska, 1992). This study will qualify the available Coronal Index data under stochastic models regarding different duration of Coronal emission cycles. This study includes the AR, MA, ARMA and ARIMA models on the Coronal Mass Ejection data which are divided into six cycles of different lengths and duration including whole Corona data. Autoregressive (AR) are the models in which value of a variable in one period is related to its values in the previous periods. In this regard, the moving Average (MA) models account for the possibility of the relationship between the variables and the residuals from the previous periods.

Autoregressive moving average combines both AR and MA terms. Lags of differenced series are referred as autoregressive and lags within forecasted data are referred as the moving average (Cooray, 2008). This study explores the Coronal emission green line cyclic data and used in Non-seasonal ARIMA models. Since the six cycles of different lengths of data are non-stationary therefore performing signify and modeling through removing the non-stationary by the series differencing (Gallager, 2012; Forouzan, 2000; Guttorp & Minin, 1995). The ARIMA modeling practiced in many research areas and confirmed the pattern of unclear data and considerable error (Lajos, 1996). The ARIMA model includes three types of parameters (p , d , q). Where p is number of autoregressive terms q is number of lagged forecast error and d is number of non- seasonal differences for stationary. The objective of these filters to end up with a white noise process which is unpredictable (Davis, Elósegui, Mitrovica & Tamisiea et al., 2004; Chatfield, 1989; and Sprott, 2003).

MATERIAL AND METHODS

In this research work Coronal emission FeXIV iron (The Green Line) data observed under stochastic methods. In this regards monthly data starting from 1944 to 2008 is distributed among six durations namely cycles (18, 19, 20, 21, 22 & 23) of different lengths and peak, including the whole data and they are (1944.06-1954.08), (1954.08-1964.09), (1964.09-1976.04), (1976.04-1986.06), (1986.06-1996.03) and (1996.03-2008.09) respectively. The minimum and maximum duration of Coronal cycle is 10.1 years and 12.6 years respectively.

Stochastic Autoregressive Models

A stochastic process is relation of random variables (Max & Compute, 1997). A stochastic process is known as random process and it is a method is a collection of random variable over time or random variable representing collection of some arrangement of random values over time. These are time depend probability distribution maps and they vary either continuously or discrete with time, if they vary at discrete times, those times might be deterministic or random. This is the probabilistic part of a deterministic process. The method espoused for model selection in this study is: to check the stationary of the series and for model identification in different time series plots, ACF and PACF are constructed using actual, changes and transformed data. To transform data, Box Cox transformation is used.

After the identification of the model, different stochastic ARIMA models are fitted on the -2log (like) Associated with the selection of the model, different model validation

statistics are recommended like Root Mean Square Error (RMSE), the Mean Absolute Percentage error, Akaike Information Criterion and Final Prediction Error Criterion and Polynomial determination (R^2). These measures are computed for each applicant model and the model having smallest AIC is recommended by assuming to be closest to the unknown reality by which series is generated. Similarly graphical validation approaches are also applied e.g. Histogram, residual plots, and PACF, ACF plots of residuals for the selection of a parsimonious model. The general ARIMA time series model equation in terms of y is:

$$\hat{y}_t = \mu + \phi_1 y_{t-1} + \dots + \phi_p y_{t-p} - \theta_1 e_{t-1} - \dots - \theta_q e_{t-q} \quad (1)$$

Here $\theta_1, \theta_2, \dots, \theta_q$ are moving average parameters (of order q) and $\phi_1, \phi_2, \dots, \phi_p$ are autoregressive parameters (of order p). Here in the general equation contains negative signs in the moving average parameter (θ 's) which is the convention introduced by Box and Jenkins. When the real numbers are fit into the equation, there is no doubt; negative sign doesn't change the general theoretical properties of the model. Although it flip the algebraic signs of estimated parameters are denoted by AR (1), AR (2),..., and MA (1), MA (2),... etc..

$$\text{MA (q): } \hat{y}_t = \mu + \theta_1 e_{t-1} + \dots + \theta_q e_{t-q} \quad (2)$$

$$\text{AR (p): } \hat{y}_t = \mu + \phi_1 y_{t-1} + \dots + \phi_p y_{t-p} \quad (3)$$

In this ordinary multiple regression model, μ is the constant term, ϕ_1 is the coefficient of the first lag of y , and so on. In this study used a Non-seasonal ARIMA models. These are most appropriate models selected. Hence, ARIMA models defined on the d th difference of the original process.

Where, ARIMA (0, 1, 1) model:

$$\hat{Y}_t = \mu + Y_{t-1} - \theta_1 e_{t-1} \quad (4)$$

ARIMA (1, 1, 1) model:

$$\hat{Y}_t = \mu + Y_{t-1} + \phi_1 (Y_{t-1} - Y_{t-2}) - \theta_1 e_{t-1} \quad (5)$$

ARIMA (2, 1, 0) model:

$$\hat{Y}_t = \mu + Y_{t-1} + \phi_1 (Y_{t-1} - Y_{t-2}) + \phi_2 (Y_{t-2} - Y_{t-3}) \quad (6)$$

Stationary Tests for Autoregressive Models

Stationary is a significant feature for extracting a time series approach. A time series model is not a predictable model if the assumption of stationary is not validated. Consequently, to extract a significant time series model the data should have stochastic stationary. The most prominent step in ARIMA box Jenkins methodology is to discover the integrated order. To check whether series is stationary or to make series stationary. Numerous stationary series have identifiable patterns for ACF and PACF. The mostly time series problem meets on non stationary in practice, while the AR and, MA in the aspects of ARIMA model confirms only for a stationary time series. The sense of series must be a weakly stationary series for an ACF. The understanding of the any particular lag autocorrelation is same in any case of where we are in time. The other way to define stationary series if the one autoregressive parameter must within the interval of $-1 < y_t < 1$ (Graham, 2003; Chatfield, 1989;). For this purpose, mean was compared and variance of distinct cycle of coronal green line emission, If series y is stationary (or trend stationary), then it has tendency to return to constant (deterministically trending) mean.

Models Adequacy Tests

This section, testimony the ARIMA models using green emission line cyclic data starting from 1944 to 2008. The objective is to settle the best model among the models that has

minimized error between the Original values and estimated values. For this purpose quality of the models has been obtained by the following methods. Appropriated models were selected for which values of modified Root Mean Square Error (RMSE), Mean Absolute Percentage error (MAPE), Akaike Information Criterion (AIC) and Final Prediction Error (FPE).

Root Mean Square Error (RMSE)

$$RMSE = \sqrt{\frac{\sum_{i=1}^n (\hat{y}_i - y_i)^2}{n}} \tag{7}$$

Where n is the number of time periods.

Mean Absolute Percentage Error (MAPE)

Mean absolute percentage error evaluates the quality of the fit, while removing the scale effect and not relatively penalizing bigger errors.

$$MAPE = \frac{100}{n} \sum_{t=1}^n \frac{|y_t - \hat{y}_t|}{|y_t|} \tag{8}$$

Akaike Information Criterion (AIC)

N is the number of data points, V_n is an index related to the prediction error, or the residual sum of squares, and p define the number of parameters in the following model.

$$AIC = v_n \left(1 + \frac{2p}{N} \right) \tag{9}$$

Final Prediction Error Criterion (FPE)

The Final Prediction Error Criterion (FPE) estimates the model-fitting error when the model is used to predict new outputs. For the FPE, an optimization model is the one that minimizes the following equation:

$$FPE = v_n \left(1 + \frac{2p}{N-p} \right) \tag{10}$$

To choose a model that minimizes the FPE this represents a balance between number of parameters and the explained variance.

RESULT AND DISCUSSION

In this study time series of monthly FeXIV 530.03λ (green line corona) data have been observed from 1944 to 2008 is distributed among six cycles of different lengths and duration including whole Green line data. These six cycles have observed and stationary of each cycle by comparison of mean and variance depicted in Table 1.

Table1: Summary of Statistic for CMEs Duration

Cycle	Duration	Observations	Min	Max	Mean	Variance
Cycle 18	1944.06-1954.08	122	0.68	14.150	7.487	14.25
Cycle 19	1954.08-1964.09	121	1.370	20.790	9.463	39.10
Cycle 20	1964.09-1976.04	139	0.410	15.030	7.031	14.73
Cycle 21	1976.04-1986.06	122	1.090	18.100	8.685	25.65
Cycle 22	1986.06-1996.03	117	1.240	19.960	9.004	30.12
Cycle 23	1996.03-2008.09	150	0.020	12.850	5.902	10.17
Cycle 18-23	1944.06-2008.09	771	0.02	20.790	7.826	23.11

There was found stationary no systematic change in the mean and variance. As Mostly time series are not stationary and the AR and MA aspects of an ARIMA model refer only to a stationary time series. These cycles followed different stochastic model for as cycle 188, cycle 192 and cycle 193 has ARIMA (0,1,1) best fitted while cycle 190 and cycle 191 best fitted on ARIMA (1,1,1). Cycle 189 best fitted on ARIMA (2,1,0) and for the complete dataset is found ARIMA (1,0,1). All the models are tested according to AIC

and SBC criterion. According to the above fitted models, cycle (18,22,23) MA (1) (order 1 Moving average Modeling including 1 differencing), cycle (20,21) showing ARIMA (1,1,1) (order 1 auto regressive integrated moving average) only cycle 189 is showing AR (2) (order 2 autoregressive including 1 differencing) in overall data from 1944 to 2008 varies ARMA (1,0,1) (including AR and MA) model that has 0 difference while others cycle's settled on 1 differencing . All results are depicted in Table 2.

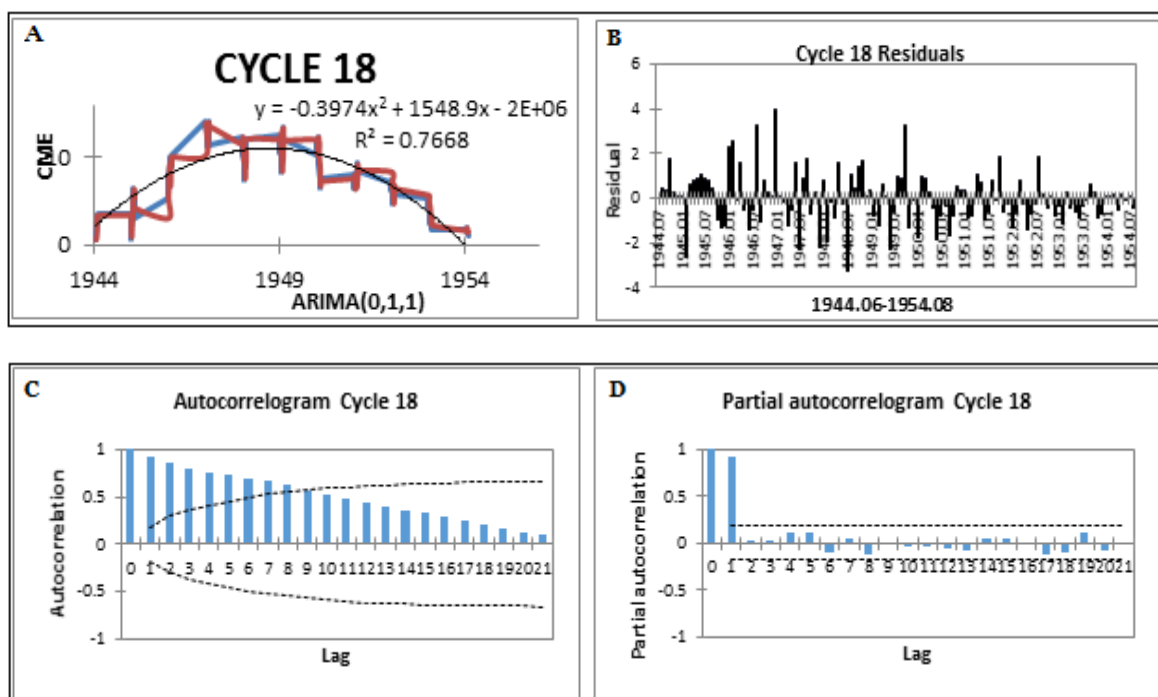
Table 2 (a) Goodness of Fit Test for CME Cycles After Optimization.

Cycle	Model	MSE	RMSE	SSE	MAPE (Diff)	MAPE
Cycle 18	ARIMA (0,1,1)	1.378414	1.174059	166.7881	103.6183	15.72037
Cycle 19	ARIMA (2,1,0)	6.5707	2.5633	788.48	186.0030836	22.1923534
Cycle 20	ARIMA (1,1,1)	4.465011	2.113057	616.1715	300.1227	44.30332
Cycle 21	ARIMA (1,1,1)	7.768228	2.787154	939.9556	300.9232	36.07252
Cycle 22	ARIMA (0,1,1)	6.264226	2.502844	726.6502	197.014	22.83514
Cycle 23	ARIMA (0,1,1)	2.320463	1.523307	345.7489	270.0241	399.183
Cycle 18-23	ARIMA (1,0,1)	4.731095	2.175108	3647.675	100.7404	100.7404

Table 2 (b) Goodness of Fit Test for CME Cycles After Optimization.

Cycle	Model	FPE	-2Log (Like)	AICC	AIC	SBC
Cycle 18	ARIMA (0,1,1)	1.378414	382.2179	386.3196	386.2179	391.8095
Cycle 19	ARIMA (2,1,0)	6.793789	566.80030836	573.00758	572.800992	581.1635
Cycle 20	ARIMA (1,1,1)	4.530193	598.7096	604.8887	604.7096	613.4913
Cycle 21	ARIMA (1,1,1)	7.897699	591.8674	598.0726	597.8674	606.2548
Cycle 22	ARIMA (0,1,1)	6.264226	542.522	546.6282	546.522	552.0292
Cycle 23	ARIMA (0,1,1)	2.320463	548.7731	552.8553	552.7731	558.781
Cycle 18-23	ARIMA (1,0,1)	4.743384	3388.181	3394.212	3394.181	3408.124

Figure 1 a Plot of Cycle 18 and Fitted ARIMA



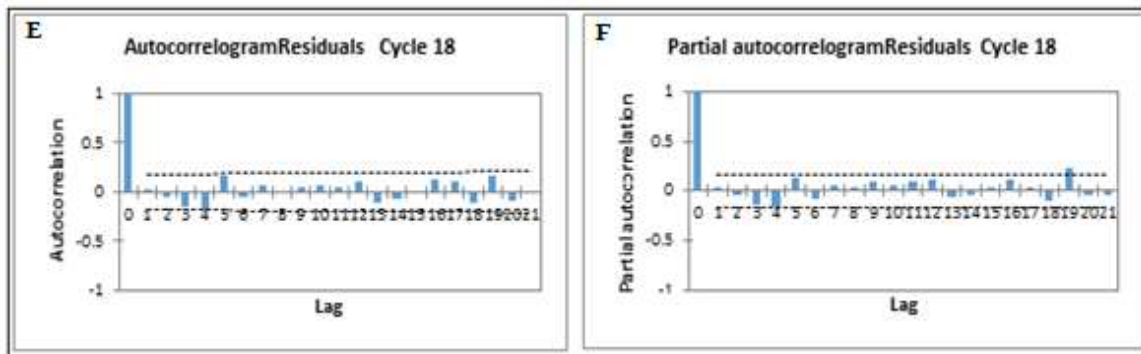


Figure 1: a: plot of cycle 18 and fitted ARIMA (0,1,1), b: Residuals plot of cycle 18, c:ACF plot of the cycle 18, d:PACF plot of the cycle 18, e: Residual of the ACF plot after applying ARIMA(0,1,1), f:Residual of PACF plot after applying ARIMA (0,1,1). label X axis number of the time lag and Y axis correlation coefficient between -1 & 1. Dotted line represent 95% confidence interval.

Figure 2 a Plot of Cycle 19 and Fitted ARIMA

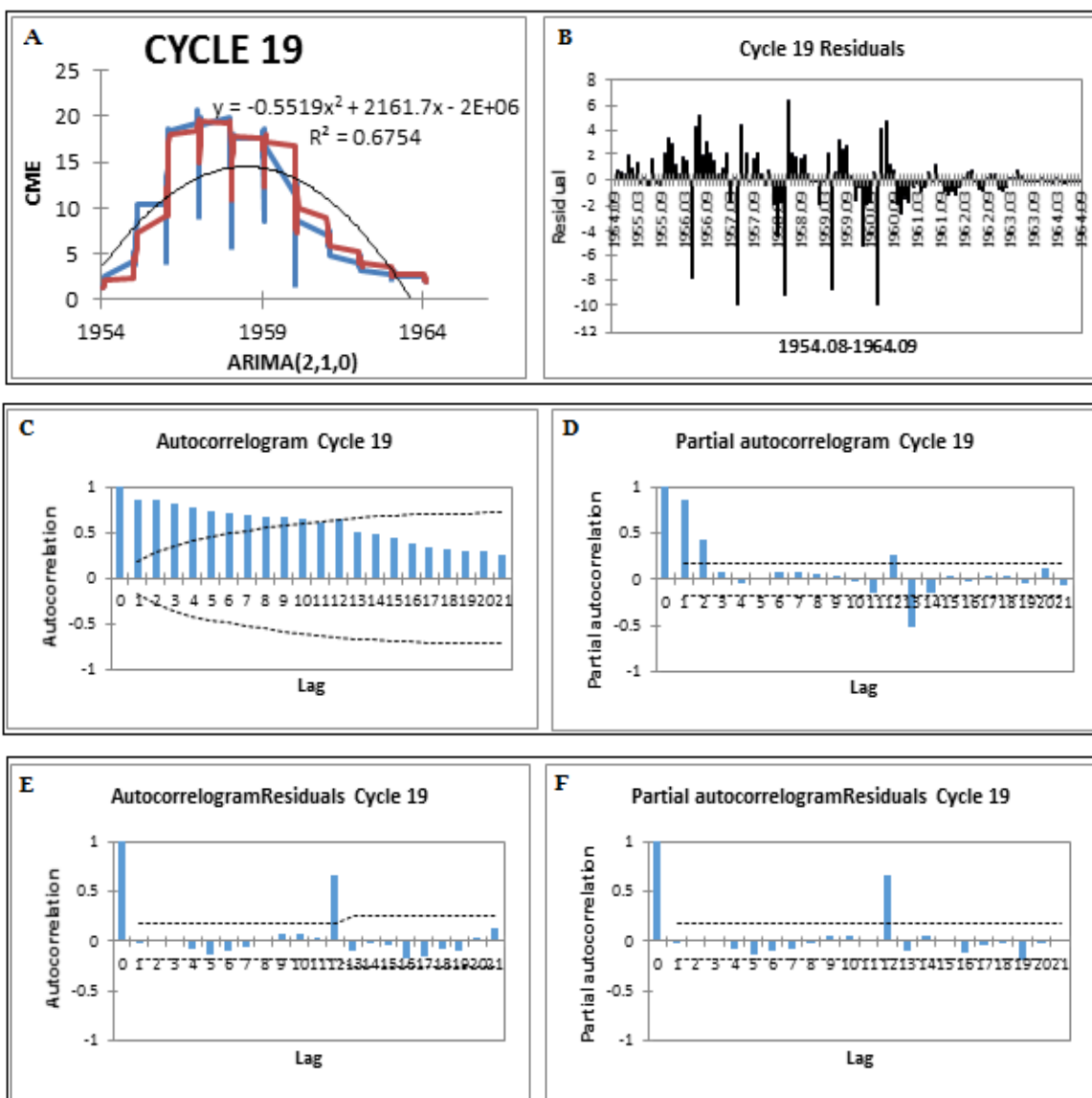


Figure 2a Plot of Cycle 19 and Fitted ARIMA (2,1,0),b: Residual plot of cycle 19,c:ACF plot of the cycle 19, d:PACF plot of cycle 189, e: Residual of the ACF plot after applying the ARIMA

(2,1,0), f:Residual of PACF plot after applying ARIMA (2,1,0). label X axis number of time lag and Y axis correlation coefficient between -1 & 1. Dotted line represent 95% confidence interval.

Figure 3 a Plot of Cycle 20 and Fitted ARIMA

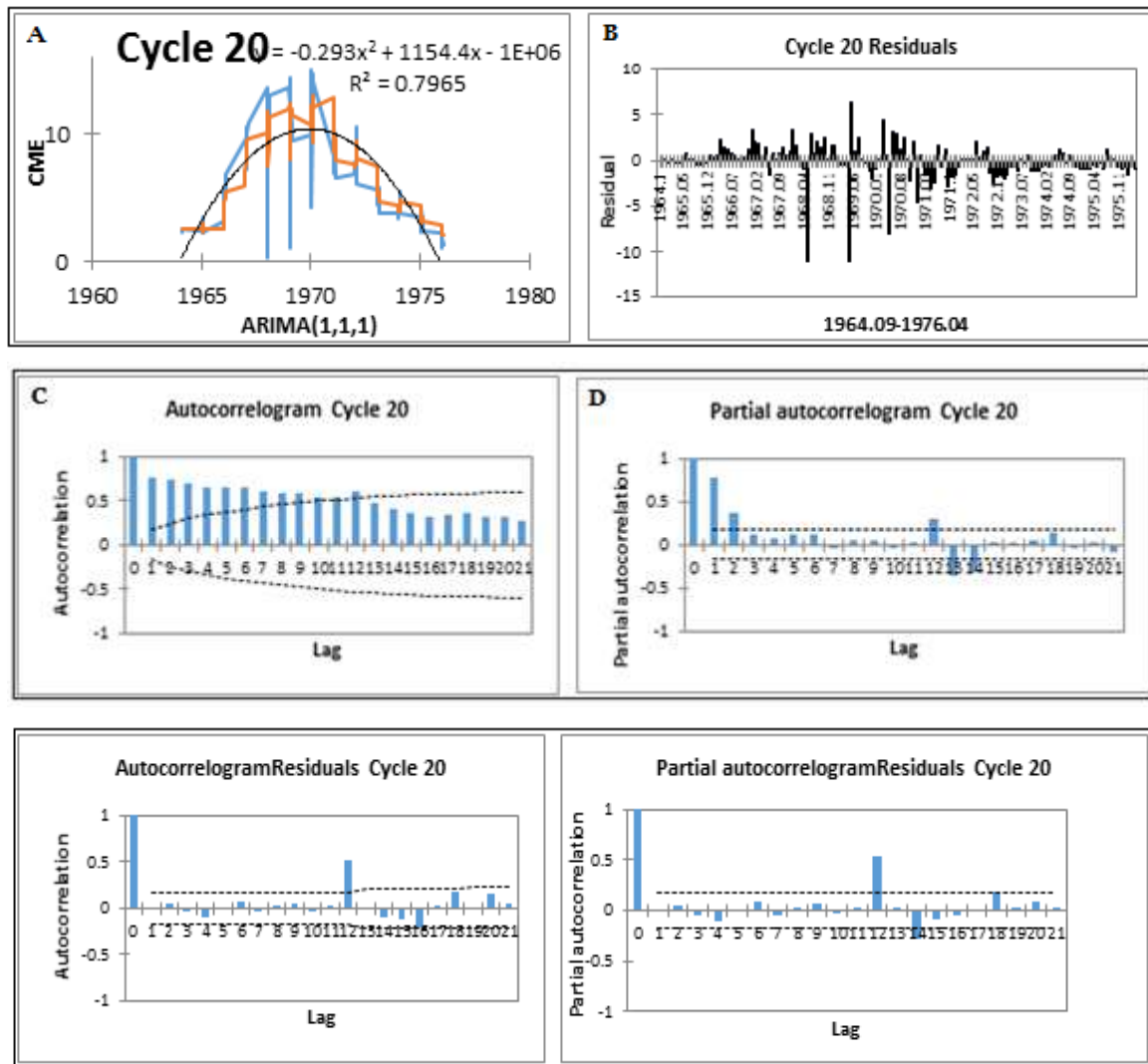
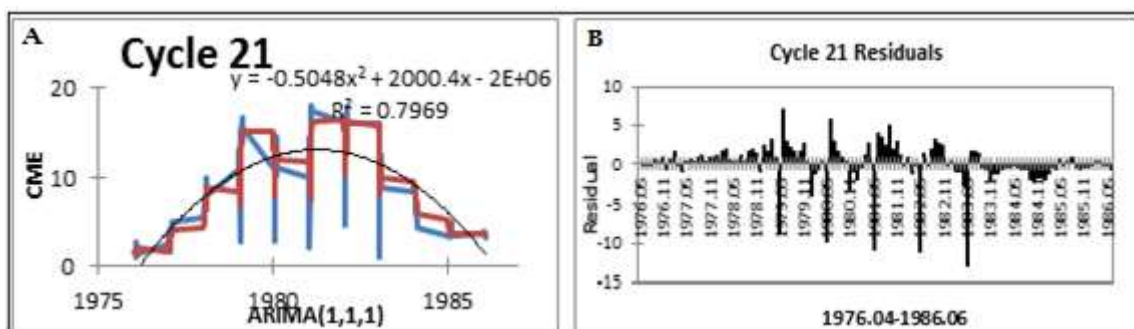


Figure 3a Plot of cycle 20 and fitted ARIMA (1,1,1), b: Residual plot of cycle 20, c:ACF plot of cycle 20, d:PACF plot of cycle 20, e: Residual of ACF plot after applying ARIMA (1,1,1), f: Residual of PACF plot after applying ARIMA (1,1,1). label X axis number of time lag and the Y axis correlation coefficient between -1 & 1. Dotted line represent 95% confidence interval.

Figure 4a Plot of Cycle 21 and Fitted ARIMA



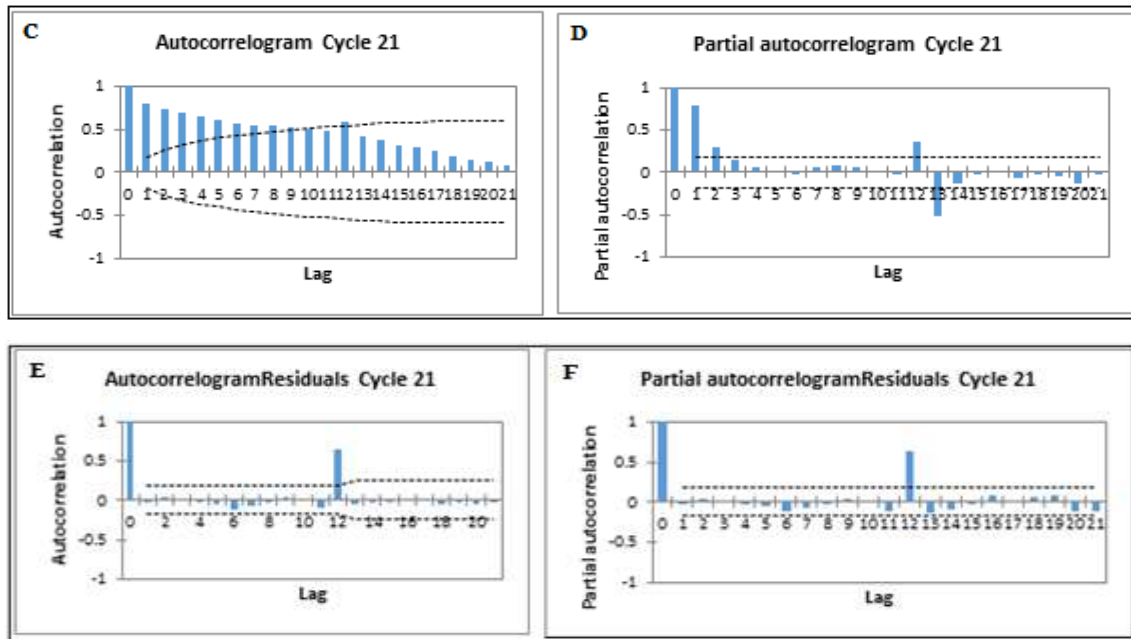


Figure 4a Plot of cycle 21 and fitted ARIMA (1,1,1), b: Residual plot of cycle 21, c:ACF plot of cycle 21, d:PACF plot of cycle 21, e: Residual of ACF plot after applying ARIMA (1,1,1), f: Residual of PACF plot after applying ARIMA (1,1,1). label X axis number of time lag and Y axis correlation coefficient between -1 & 1. Dotted line represent 95% confidence interval.

Figure 5a Plot of Cycle 22 and Fitted ARIMA

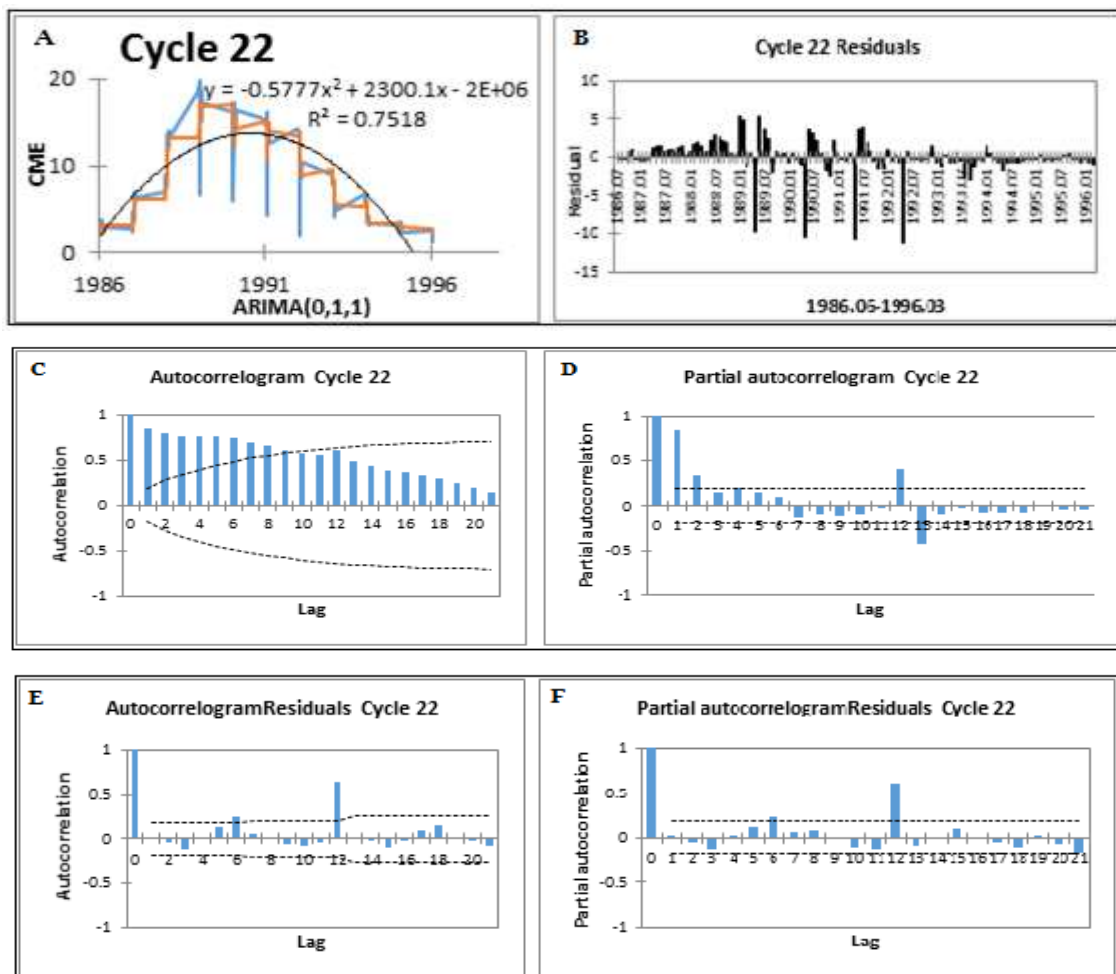


Figure 5a Plot of cycle 22 and fitted ARIMA (0,1,1), b: Residual plot of cycle 22, c:ACF plot of cycle 22, d:PACF plot of cycle 22, e: Residual of ACF plot after applying ARIMA (0,1,1), f: Residual of PACF plot after applying ARIMA (0,1,1). label X axis number of time lag and Y axis correlation coefficient between -1 & 1. Dotted line represent 95% confidence interval.

Figure 6a Plot of Cycle 23 and Fitted ARIMA

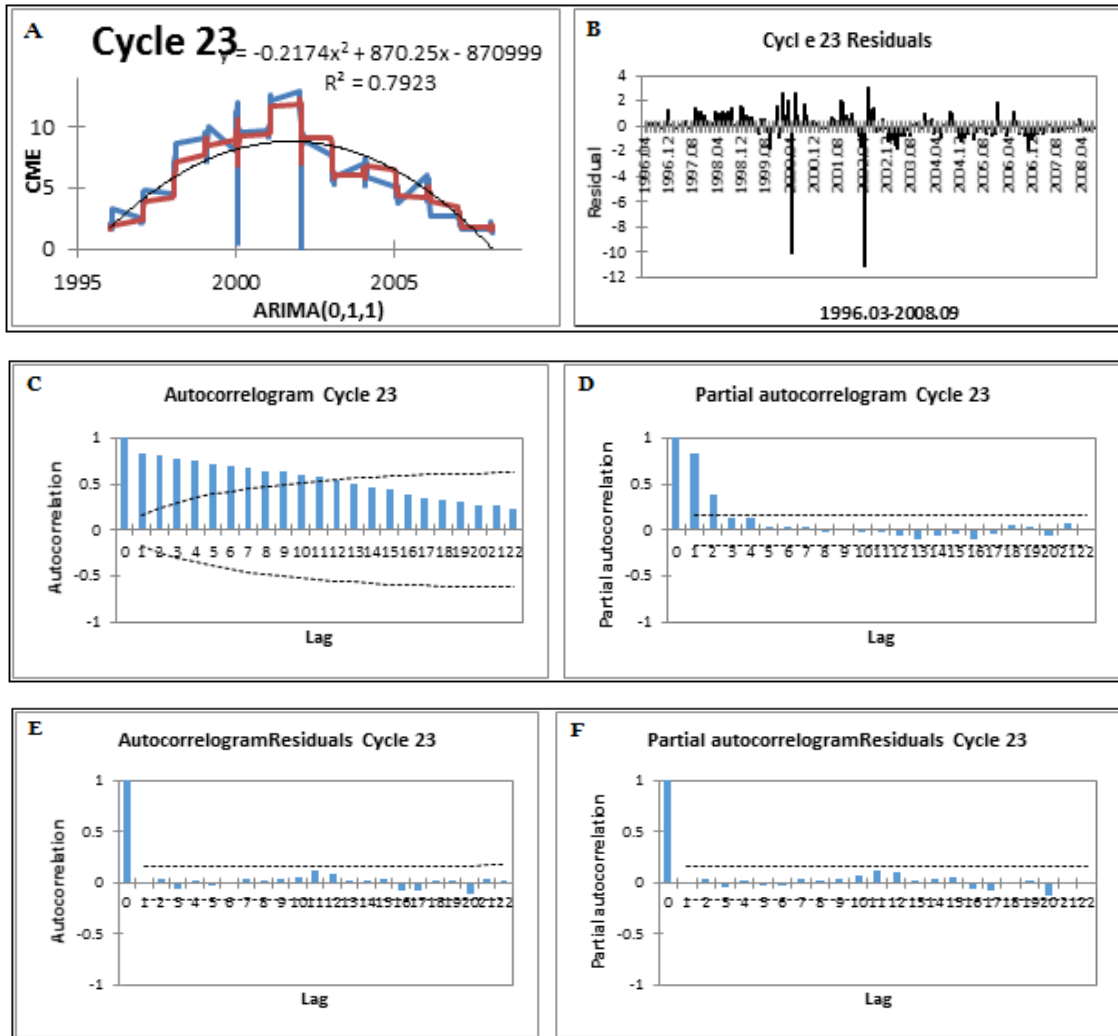
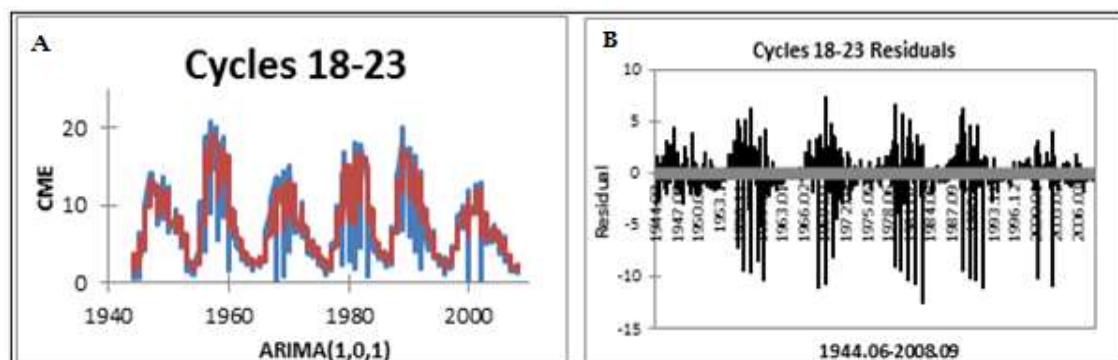


Figure 6a Plot of cycle 23 and fitted ARIMA (0,1,1), b: Residual plot of cycle 23, c:ACF plot of cycle 23, D:PACF plot of cycle 23, e: Residual of ACF plot after applying ARIMA (0,1,1), f: Residual of PACF plot after applying ARIMA (0,1,1). label X axis number of time lag and Y axis correlation coefficient between -1 & 1. Dotted line represent 95% confidence interval.

Figure 7a Plot of Cycle 18-23 and Fitted ARIMA



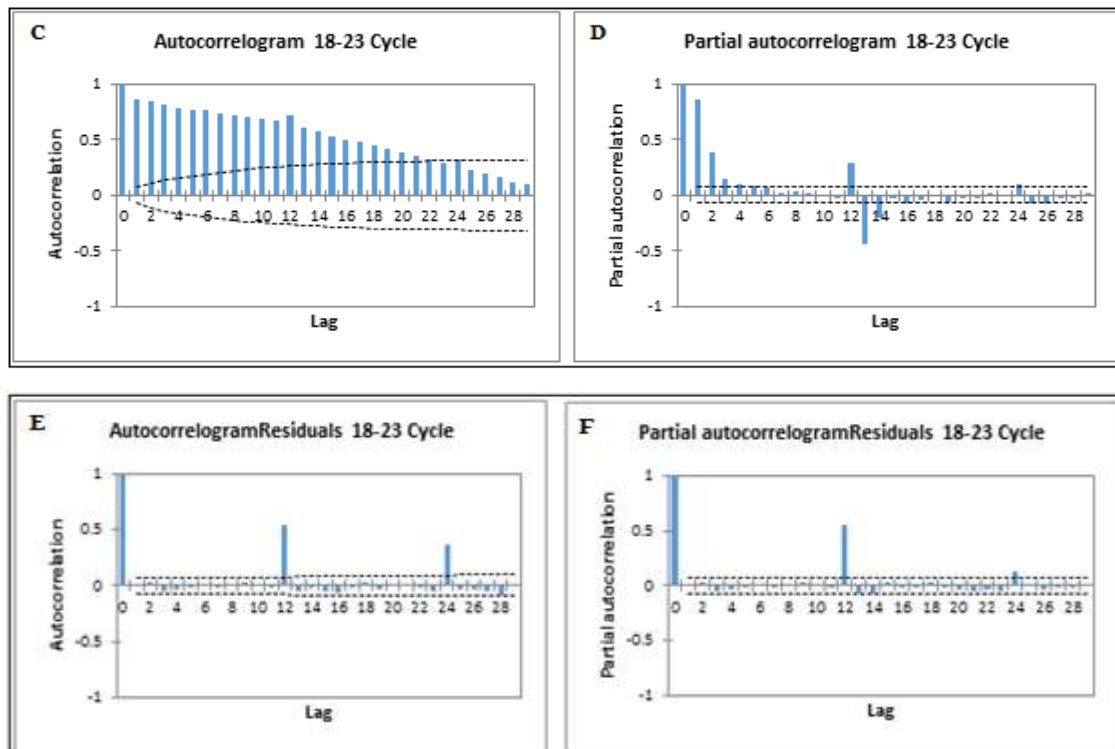


Figure 7a Plot of cycle 18-23 and fitted ARIMA (1,0,1), b: Residual plot of cycle 18-23, c: ACF plot of cycle 18-23, d: PACF plot of cycle 18-23, e: Residual of ACF plot after applying ARIMA (1,0,1), f: Residual of PACF plot after applying ARIMA(1,0,1). label X axis number of time lag and the Y axis correlation coefficient between -1 & 1. Dotted line represent 95% confidence interval.

Further, we determined by analysis of autocorrelation and partial autocorrelation. Figure from 1to7 (c) and (d) showing non seasonal parameter (p, d, q) required for settlement of the model. In significant spikes cut through lag 1 and lag 12 of each cycle except lag 9 in cycle 18 and lag 24 in cycle 18-23 was observed in the plot of ACF. While in case of PACF, partial autocorrelation is dropping after lag 1 and more gradually over time, then compare these two lags of ACF of original data. For best adequacy of the model utilized both ACF and PACF to investigate setting of models on the cycles and complete dataset from 1944 to 2008. For this purpose, lowest Akaike Information Criterion and Mean Absolute percent error (MAPE) value of different cycles has competed in corresponding to different choices of p, d and q for the ARIMA models. All MAPE and AIC value depicts in TABLE 2 (b).

Table 2 (b) AIC and MAPE values of different duration of CME cycles.

Cycle	MAPE	AIC
Cycle 18 (0,1,1)	15.72037	386.2179
Cycle 19 (2,1,0)	22.19235344	572.8009692
Cycle 20 (1,1,1)	44.30332	604.7096
Cycle 21 (1,1,1)	36.07252	597.8674
Cycle 22 (0,1,1)	22.83514	546.522
Cycle 23 (0,1,1)	399.183	552.7731

For example cycle 18 has best fitted on ARIMA (0,1,1) among the models had both lowest values are AIC (386.3196) and MAPE (15.72037). A Similar process has adapted to other cycles. In residual analysis plot of ACF, PACF also drop at lag 1 and residual correlation

inside the 95% confidence limit. The appropriate model residuals are likely to be random and close to zero. All residual plots depicted in the figure 1 to 7 (e) and (f). In this study figure showed some lags are zero, some are significantly differ from zero and tapering (one or two) lag outside the 95% confidence. There is no evidence to reject the model also, in connection of the residual analysis Table 2 (c) showed Root mean square error (RMSE) values vary final prediction error (FPE) values.

Table 2 (c) RMSE and FPE Values of Different Duration CME Cycles

Cycle	RMSE	FPE
Cycle18 (0,1,1)	1.174059	1.378414
Cycle19 (2,1,0)	2.5633	6.793477891
Cycle20 (1,1,1)	2.113057	4.530193
Cycle21 (1,1,1)	2.787154	7.897699
Cycle22 (0,1,1)	2.502844	6.264226
Cycle23 (0,1,1)	1.523307	2.320463

For example, cycle 18 had both the corresponding lowest RMSE (1.174059) and the FPE (1.378414) values. Similarly cycle 21 had both corresponding highest RMSE (2.787154) and FPE (7.897699) values. It is directly proportional and also valid for other cycles and predictive power of ARIMA fitted models. In the end the all Model parameter coefficient and polynomial estimated, and standard deviation calculated by estimation method or from Fisher's information matrix (Hessian) with estimation of asymptotically standard deviations. For each cycle coefficient, standard deviation and confidence interval is depicted in Table 3.

Table 3 Coefficient Values of Parameter, Hessian & ASE Confidence Interval of Each Model

Cycle	Model	P	Value	HSE	LB95%	UB95%	ASE	LB95%	UB95%
Cycle 18	(0,1,1)	MA (1)	-0.043	0.098	-0.235	0.149	0.091	-0.221	0.135
Cycle 19	(2,1,0)	AR (1)	-0.581	0.090	-0.757	-0.404	0.090	-0.758	-0.404
		AR (2)	-0.135	0.090	-0.310	0.041	0.090	-0.312	0.043
Cycle 20	(1,1,1)	AR (1)	0.076	0.122	-0.163	0.314	0.127	-0.172	0.324
		MA (1)	-0.710	0.084	-0.875	-0.545	0.089	-0.885	-0.535
Cycle 21	(1,1,1)	AR(1)	0.172	0.161	-0.144	0.487	0.152	-0.125	0.469
		MA(1)	-0.692	0.122	-0.932	-0.452	0.111	-0.910	0.469
Cycle 22	(0,1,1)	MA(1)	-0.620	0.066	-0.749	-0.491	0.073	-0.763	-0.477
Cycle 23	(0,1,1)	MA(1)	-0.630	0.062	-0.751	-0.509	0.06	-0.755	-0.506
Cycle(18-23)	(1,0,1)	AR(1)	0.977	0.008	0.961	0.994	0.008	0.961	0.993
		MA(1)	-0.546	0.034	-0.613	-0.479	0.033	-0.610	-0.482

(P: Parameter. HSE: Hessian Standard Error, LD: Lower Bound, UB: Upper Bound, ASE: Asympt: Standard Error)

The Table showed the Hessian standard error and asymptotic standard error is slightly changed (ignorable) as well as in the confidence interval. It means the fitness of the model.

CONCLUSION

This study concludes the settlement of the six Coronal FeIV530.03λ data set cycle's from 1944 to 2008. As a conclusion, we can say that the selected stochastic model on cycle 18,22,23 is an ARIMA (0,1,1) and having ordered 1 Moving Average (MA) model while cycle 20 and cycle 21 has settled on same ARIMA (1,1,1) model except cycle 19 settled on ARIMA (2,1,0) and having ordered 2 Autoregressive (AR) model. All cycle's settled on linear differencing trend and complete green line Corona cycle settled on ARIMA (1, 0, 1) ARMA model. As mostly natural phenomena's are non-stationary and they can be best fitted with the stochastic model. However, the ARIMA models are being selected for this astronomical data and variables for similar cycles. The study may useful to understand

the stochastic behavior of CME in future. The work done in this research paper can also be established for other emission line Corona (like red line corona) data by fitting the same stochastic models. For providing the Coronal index monthly data the World Data Center (WDC) and NOAA are acknowledged.

REFERENCES

- Akhter, M. F., Abbas, S., & Hassan, D. (2018). Study of Coronal Index Time Series Solar Activity Data in the Perspective of Probability Distribution. *Proceeding of the Pakistan Academy of Sciences*, (55).
- Akhter, M. F., Abbas, S., & Hassan, D. (2019). The relationship of periodic behaviour between coronal index cycles and associated ENSO by using Markov process. *Astrophysics and Space Science*, 364(7), 107.
- Chatfield, C. D. (1989). *Time series analysis: An introduction*. The Chapman and Hall, London.
- Cooray, K. (2008). *Applied Time Series, Analysis and Forecasting*, Narosa publishing House, New Delhi, India.
- Davis, J. L., Elósegui, P., Mitrovica, J. X., & Tamisiea, M. E. (2004). Climate-driven deformation of the solid Earth from GRACE and GPS. *Geophysical Research Letters*, 31 (24).
- Ebert, R. W., McComas, D. J., Elliott, H. A., Forsyth, R. J., & Gosling, J. T. (2009). Bulk properties of the slow and fast solar wind and interplanetary coronal mass ejections measured by Ulysses: Three polar orbits of observations. *Journal of Geophysical Research: Space Physics*, (1978–2012), 114 (A1).
- Forouzan, B. A. (2000). *Data communication and networking*. Second Edition, McGraw-Hill.
- Gallager, R. G. (2012). *The Stochastic Processes: The Theory for Applications of the real Draft*.
- Gopalswamy, N., Yashiro, S., Kaiser, M. L., Howard, R. A., & Bougeret, J. L. (2001). Radio signatures of coronal mass ejection interaction: coronal mass ejection cannibalism? *The Astrophysical Journal Letters*, 548 (1), L91.
- Graham B. (2003). *Statistics of Earth Science Data*. Springer-Verlag Berlin Heidelberg N.Y.
- Guttorp, P., & Minin, V. N. (1995). *The Stochastic modeling of scientific data*. The CRC Press.
- Howard, R. A. (2006). A historical perspective on coronal mass ejections. *Geophysical Monograph-American Geophysical Union*, 165, 7.
- KP, A. B. (2014). *Coronal Mass Ejections from the Sun-Propagation and Near Earth Effects* (Doctoral dissertation, Indian institute of science education and research Pune).
- Lajos T. (1996). *The Stochastic Processes*. The Science Paperbacks and Methuen and Co. Ltd.
- Mariska, J. T. (1992). *The solar transition region* (Vol. 23). The Cambridge University Press.
- Max, L., & Compute, M. L. T. (1997). *The Introduction to the Stochastic Processes*. Press release.

Prabhakar, M., Raju, K. P., & Chandrasekhar, T. (2013). Analysis of the solar coronal green line profiles from eclipse observations. arXiv preprint arXiv:1307.0352.

Schwenn, R., Inhester, B., Plunkett, S. P., Epple, A., Podlipnik, B., Bedford, D. K., & Lamy, P. L. (1997). First view of the extended green-line emission corona at Solar activity minimum using the LASCO-C1 coronagraph on SOHO. In *The First Results from SOHO* (pp. 667-684). Springer Netherlands.

Sprott, J. C. (2003). *Chaos and time-series analysis* (Vol. 69). Oxford: Oxford University Press. T.M.J.A.

Wang, Y. M., Sheeley Jr, N. R., Hawley, S. H., Kraemer, J. R., Brueckner, G. E., Howard, R. A., & Schwenn, R. (1997). The green line corona and its relation to the photospheric magnetic field. *The Astrophysical Journal*, 485 (1), 419.